Supporting Information

A comprehensive investigation of condensation of furanic platform molecules to diesel precursors over sulfonic acid functionalized silica supports

Mahlet N. Gebresillase[1], Raghavendra Shavi, Jeong Gil Seo*

Department of Energy Science Technology, Myongji University, Myongji-ro 116, Nam-dong, Cheoin-gu, Yongin-si, Gyeonggi-do 449-728, South Korea

*Corresponding author.

E-mail address: jgseo@mju.ac.kr (J.G. Seo)

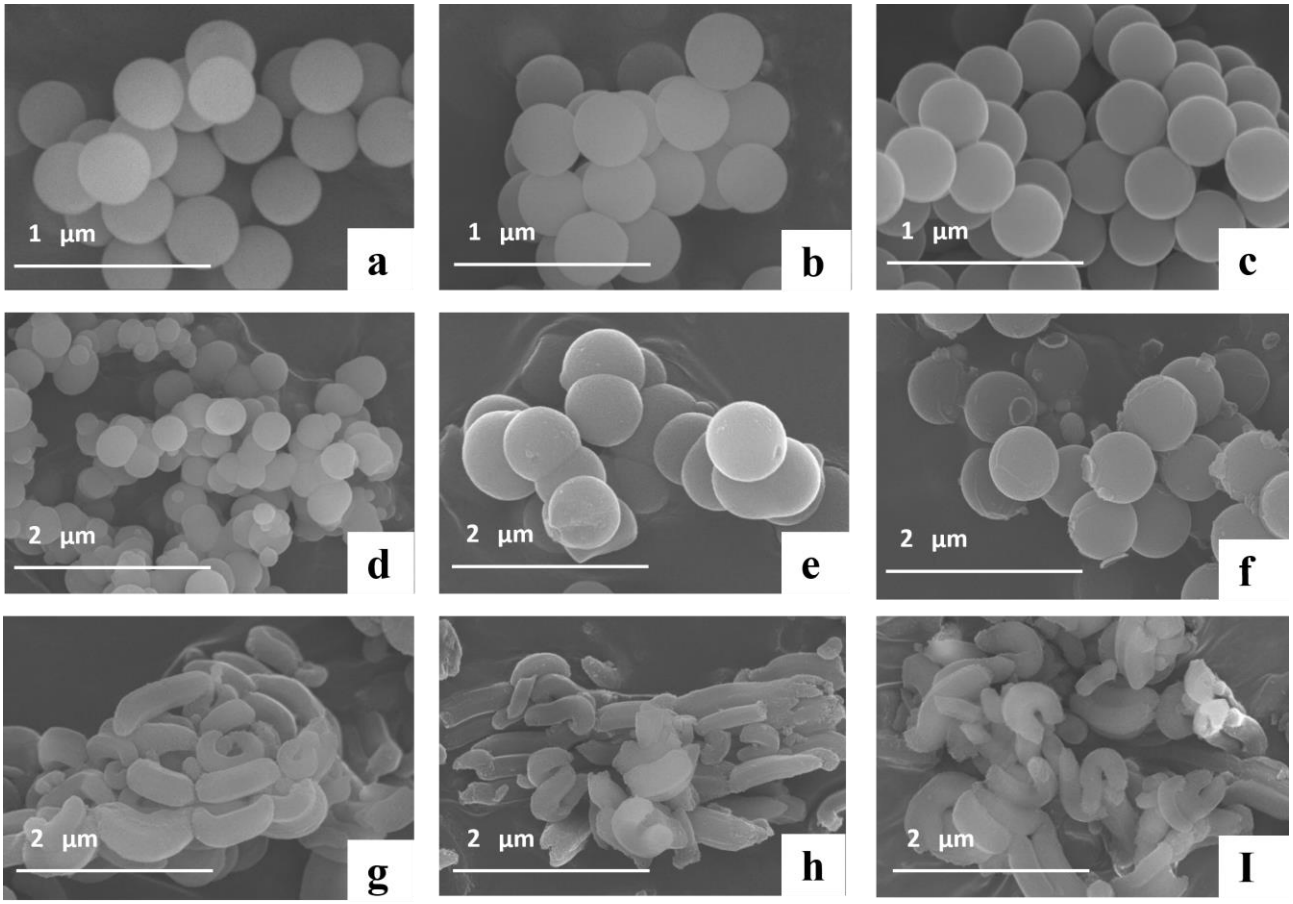

Figure S1: SEM images of NP (a), NPSO_3H (b), NPAPSO_3H (c), MCM-41 (d), MCM-41SO_3H (e), MCM-41APSO_3H (f), SBA-15 (g), SBA-15SO_3H (h), and SBA-15APSO_3H (I).

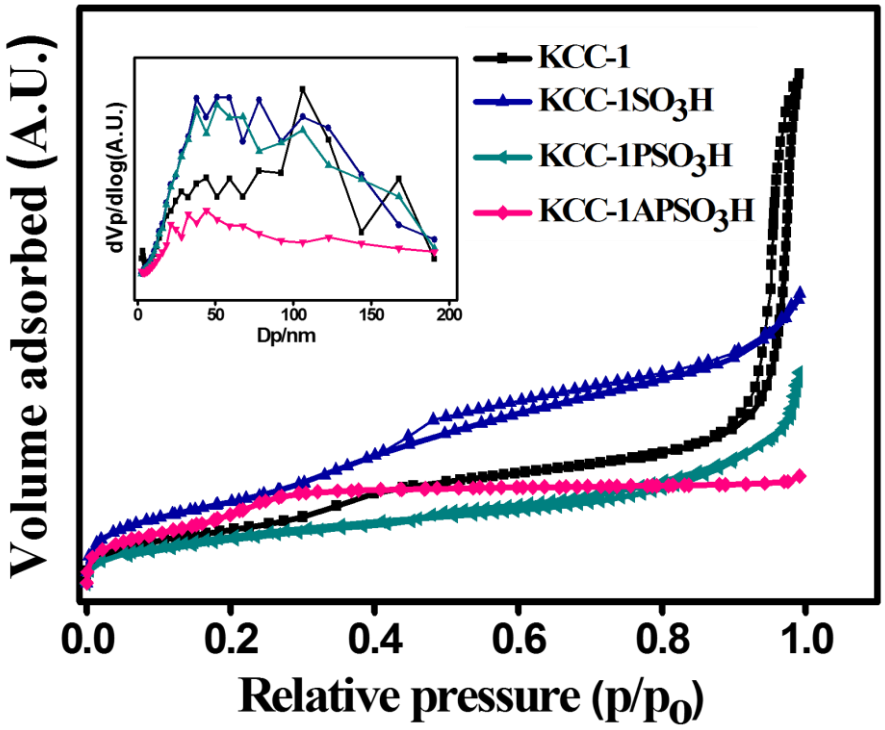

Figure S2: N_2 Adsorption-desorption isotherms (pore size distribution in inset) of KCC-1, KCC-1SO_3H, KCC-1 PSO_3H and KCC-1$APSO_3H$.

In the FT-IR spectra of KCC-1, KCC-1SO_3H, KCC-1PSO_3H, and KCC-1$APSO_3H$, the asymmetric Si—O—Si stretching from 1,200 to 1,000 cm^{-1} and OH stretch from 3,600 to 3,000 cm^{-1} showed broad absorption band. The two peaks at 880 cm^{-1} and 450 cm^{-1} are contributed by the symmetric stretching of Si—O—Si and Si—O—Si bending, respectively. As for the sulfuric acid functional groups only, the FT-IR absorption range of the O=S=O asymmetric and symmetric stretching peaks lay around 1110 and 1250 cm^{-1}, respectively, overlapping with the broad stretching band of Si–O–Si. The S–O stretching mode lies about 574 cm^{-1}, and the O–Si–O bending from KCC-1$APSO_3H$ lies about 460 cm^{-1}. The catalysts KCC-1PSO_3H, and KCC-1$APSO_3H$ show characteristic peaks for the stretching vibrations of aliphatic C–H bonds around 2960 cm^{-1} and S—C stretching around 600 cm^{-1}. The peak at 1650 cm^{-1} represents the water.

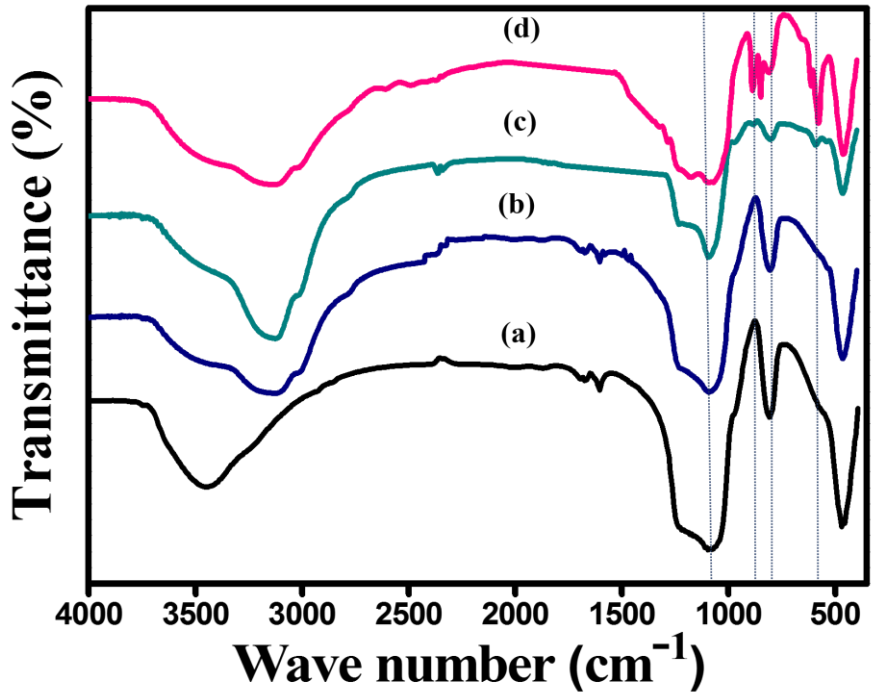

Figure S3: FTIR spectra of KCC-1 (a), KCC-1SO_3H (b), KCC-1PSO_3H (c) and KCC-1$APSO_3H$ (d).

Only a negligible weight loss of 2.4% is detected. The TGA plot of all the catalysts supported on KCC-1 confirm the incorporation of organic functionality in the silica framework. The sharp weight loss below 150 ^{0}C corresponds to the surface physiosorbed water. The additional weight loss between the temperatures 150-450 ^{0}C can be attributed to the loss of organic functionality. The weight loss increase from KCC-1SO_3H to KCC-1APSO_3H indicates the presence of additional organic moieties (alkyl chain).

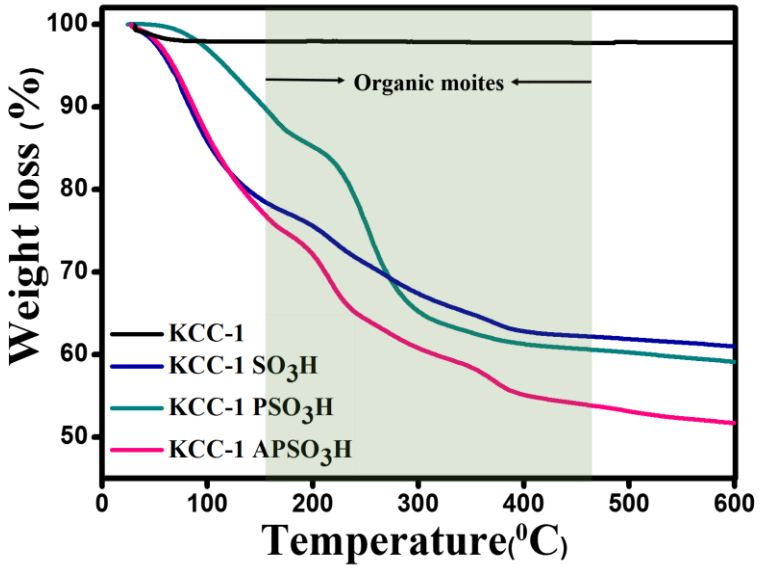

Figure S4: TGA diagram of KCC-1, KCC-1SO_3H, KCC-1PSO_3H and KCC-

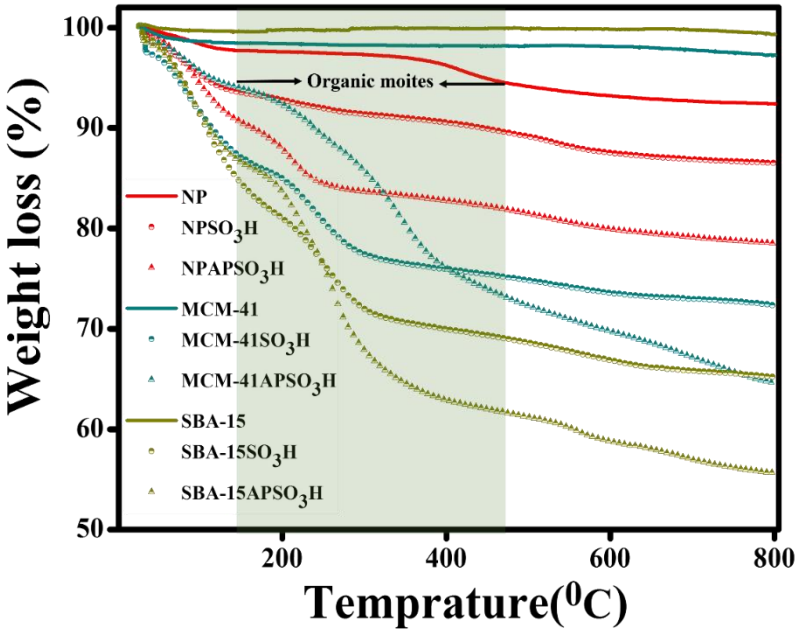

Figure S5: TGA diagram of NP, $NPSO_3H$, $NPAPSO_3H$, MCM-41, $MCM\text{-}41SO_3H$, MCM-41, $APSO_3H$, SBA-15, $SBA\text{-}15SO_3H$, and $SBA\text{-}15APSO_3H$.

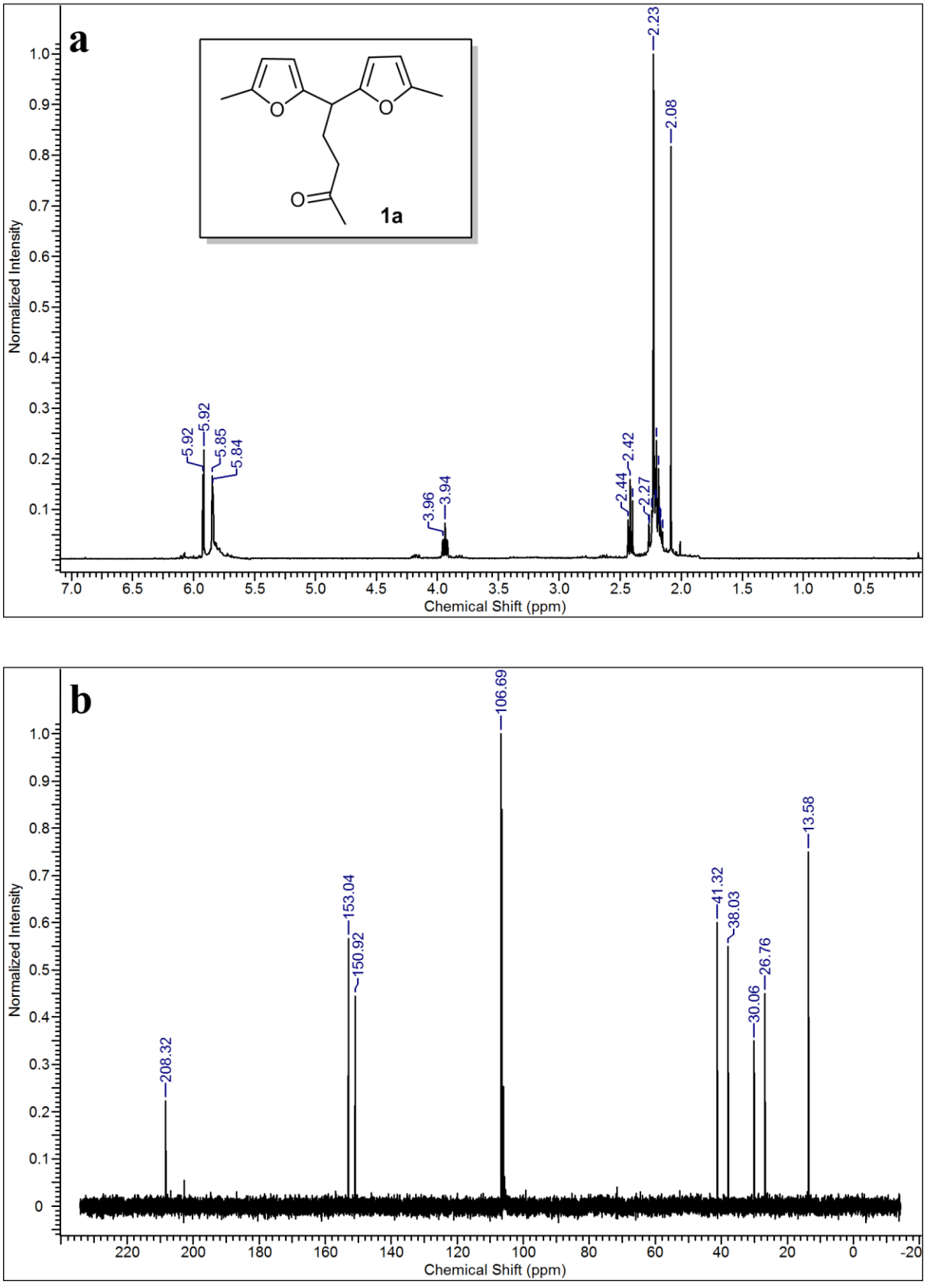

Figure S6: ^{1}H and ^{13}C NMR spectra of the 1a produced by the self-condensation of 2-MF.

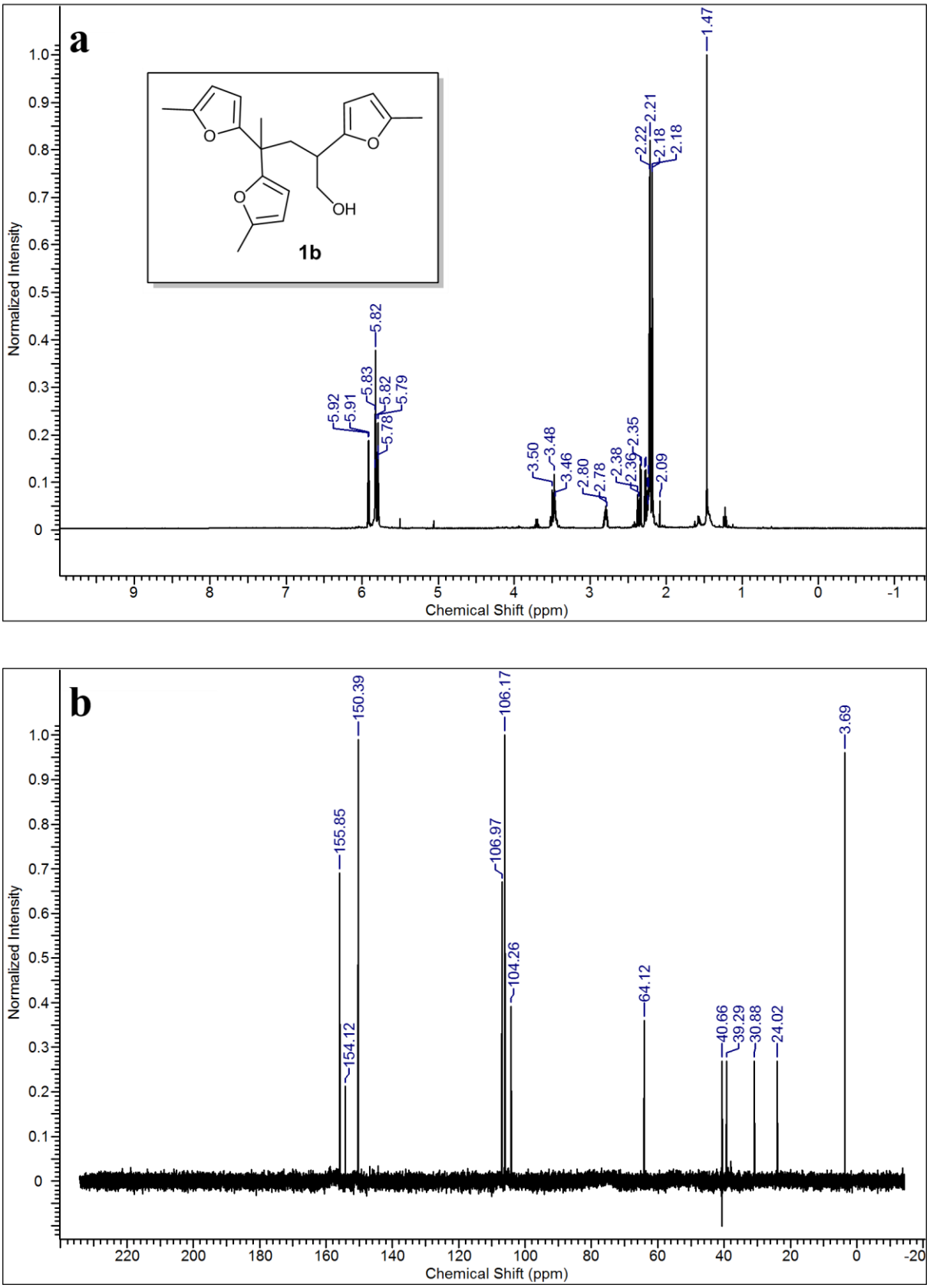

Figure S7: ^{1}H and ^{13}C spectra NMR of the 1b produced by the self-condensation of 2-MF.

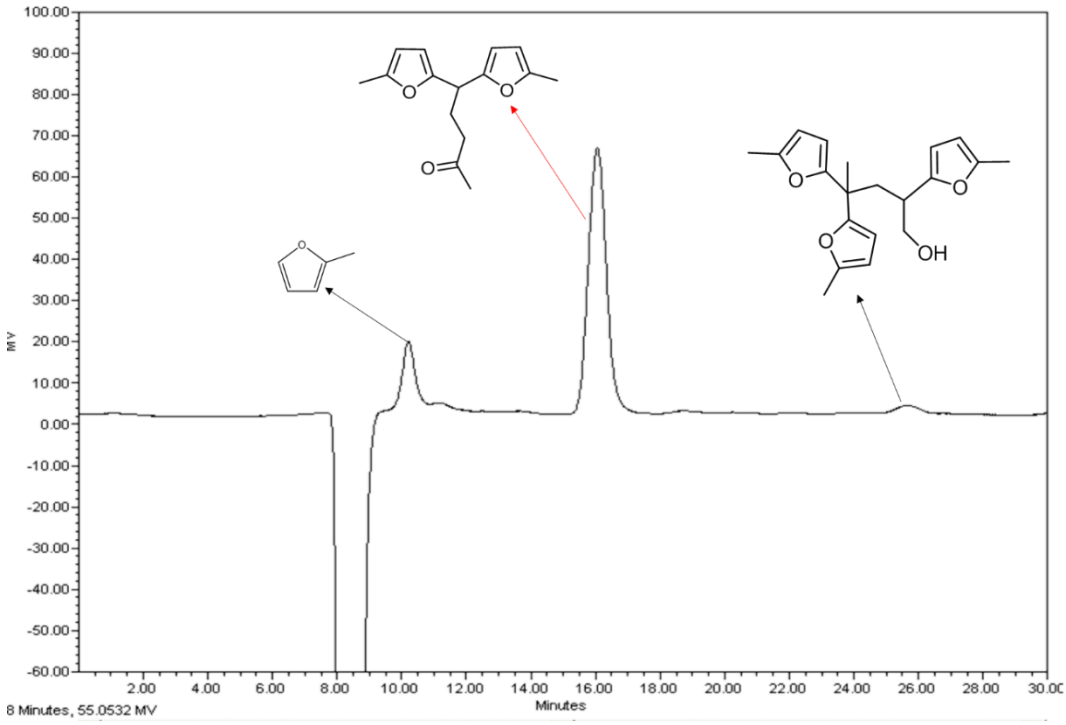

Figure S8: HPLC chromatogram of the liquid products from the self-condensation of 2-MF.

Table S1: Elemental Analysis data of the KCC-1 based catalysts

	C(wt%)	H(wt%)	S(wt%)
KCC-1SO_3H	0.1518	0.9712	3.8219
KCC-1PSO_3H	1.1675	1.2449	2.8694
KCC-1APSO_3H	1.6902	1.8851	5.5207

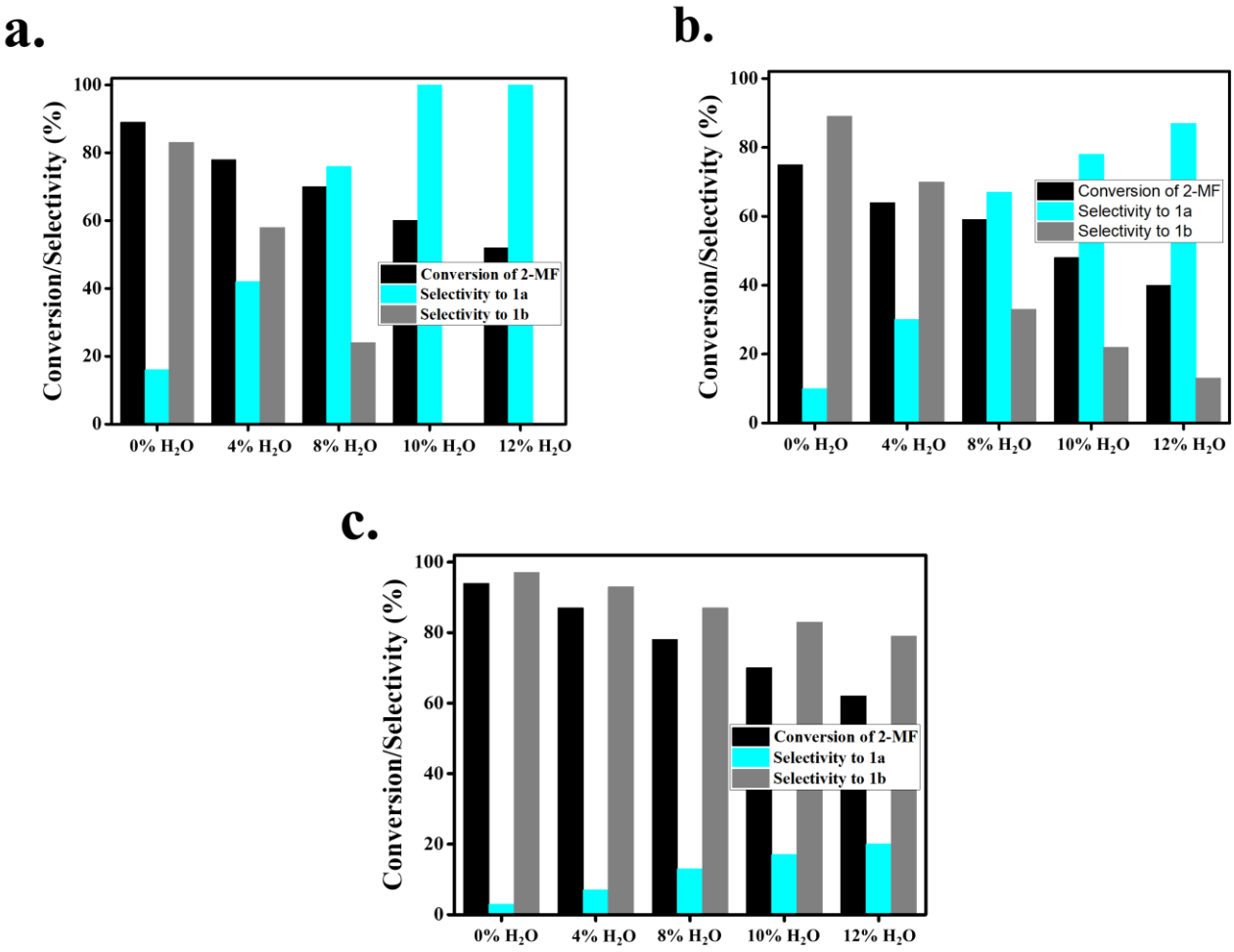

Figure S9: The effect of water on conversion of 2-MF and selectivity to 1a and 1b over a. KCC-1SO_3H b. Amberlyst-15 and c. Nafion-212.

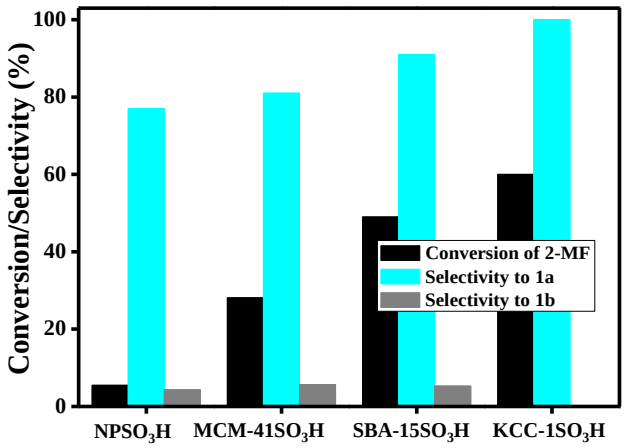

Figure S10: The effect of support morphology on conversion and selectivity. 2-MF (10 g) and catalyst (3 wt %) were condensed with an addition of water (10 wt %) at 85 ^{0}C for 48 h.

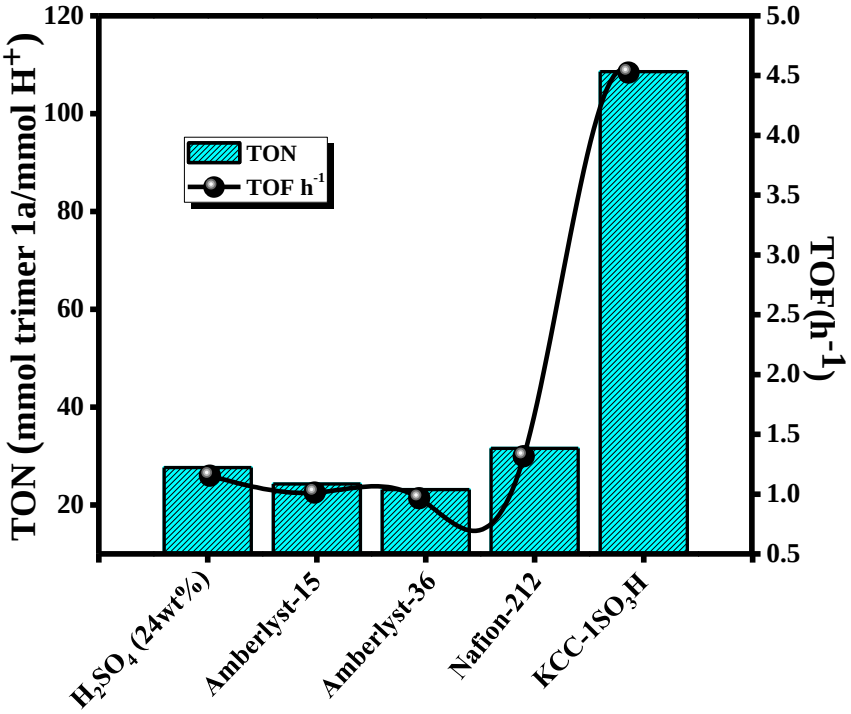

Figure S11: TON and TOF calculated from the yield after 24h reaction**.** 2-MF (10 g) and catalyst (3 wt%) were condensed with an addition of water (10 wt%) at 85 ^{0}C.

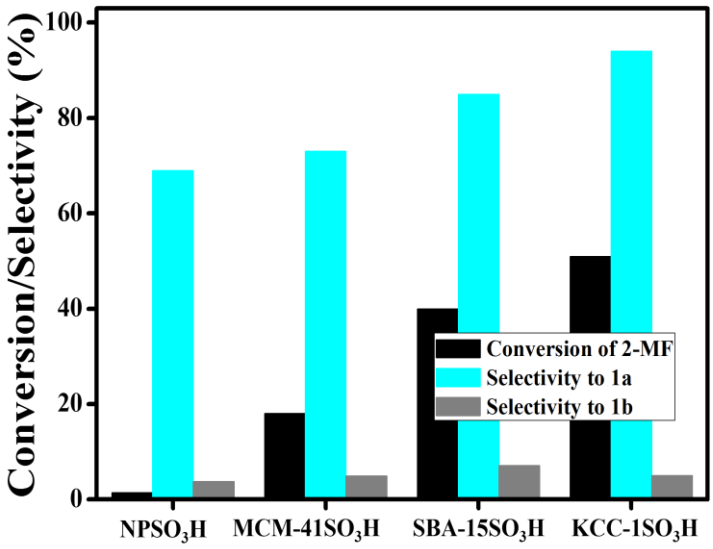

Figure S12: Self-condensation of 2-MF using recycled NP, MCM-41, SBA-15 and KCC-1 supported catalysts (reaction time = 48 h). 2-MF (10 g) and catalyst (3 wt%) were condensed with an addition of water (10 wt%) at 85^{0}C.

Table S2: Physicochemical properties of the recycled catalysts

Catalyst	[a] S_{BET}(m^2g^{-1})	% Change in S_{BET}	[a] V_{total} (cm^2g^{-1})	% Change in V_{total} (cm^2g^{-1})	[b] Acidic amount (mmolg-1)
Recycled catalyst from the Self-condensation reaction					
RNPSO$_3$H	2.4	84.8	0.03	26.8	0.2
RMCM-41SO$_3$H	187	56.8	0.10	60.7	0.45
RSBA-15SO$_3$H	205	53.4	0.13	66.7	0.78
RKCC-1SO$_3$H	243	36.8	0.71	39.3	1.01
Recycled catalyst from the Cross-condensation reaction of 2-MF and FUR					
RNPAPSO$_3$H	4.1	50	0.01	34.6	0.10
RMCM-41APSO$_3$H	163	20	0.13	47.3	0.47
RSBA-15APSO$_3$H	178	16.8	0.19	34.4	0.76
RKCC-1APSO$_3$H	206	8.4	0.75	7.4	0.99
Recycled catalyst from the Cross-condensation reaction of 2-MF and n-butanal					
RNPAPSO$_3$H	4.2	48.7	0.01	38.4	0.11
RMCM-41APSO$_3$H	161	21.0	0.11	52.6	0.74
RSBA-15APSO$_3$H	176	17.7	0.17	41.3	0.45
RKCC-1APSO$_3$H	209	7.1	0.73	9.8	0.97
Recycled catalyst from the Cross-condensation reaction of 2-MF and 2-pentanone					
RNPAPSO$_3$H	3.7	54.8	0.01	46.1	0.09
RMCM-41APSO$_3$H	124	37.2	0.11	63.1	0.41
RSBA-15APSO$_3$H	148	30.8	0.14	51.7	0.68
RKCC-1APSO$_3$H	207	8	0.71	12.3	0.91

[a] As measured by BET

[b] From titration

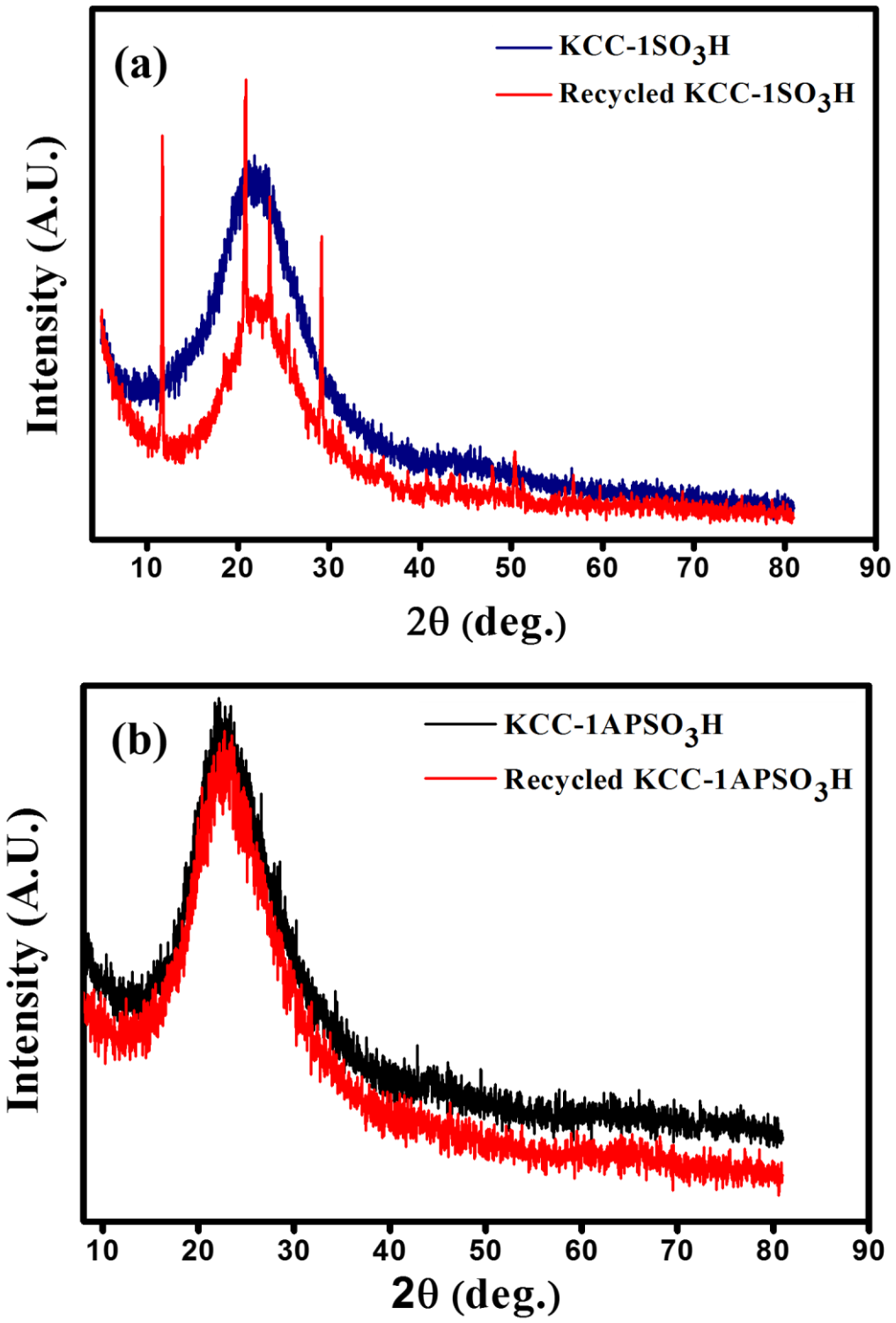

Figure S13: XRD spectrum of fresh and recycled KCC-1SO_3H from the self-condensation reaction (a) and KCC-1APSO_3H from the cross-condensation of 2-MF and FUR (b).

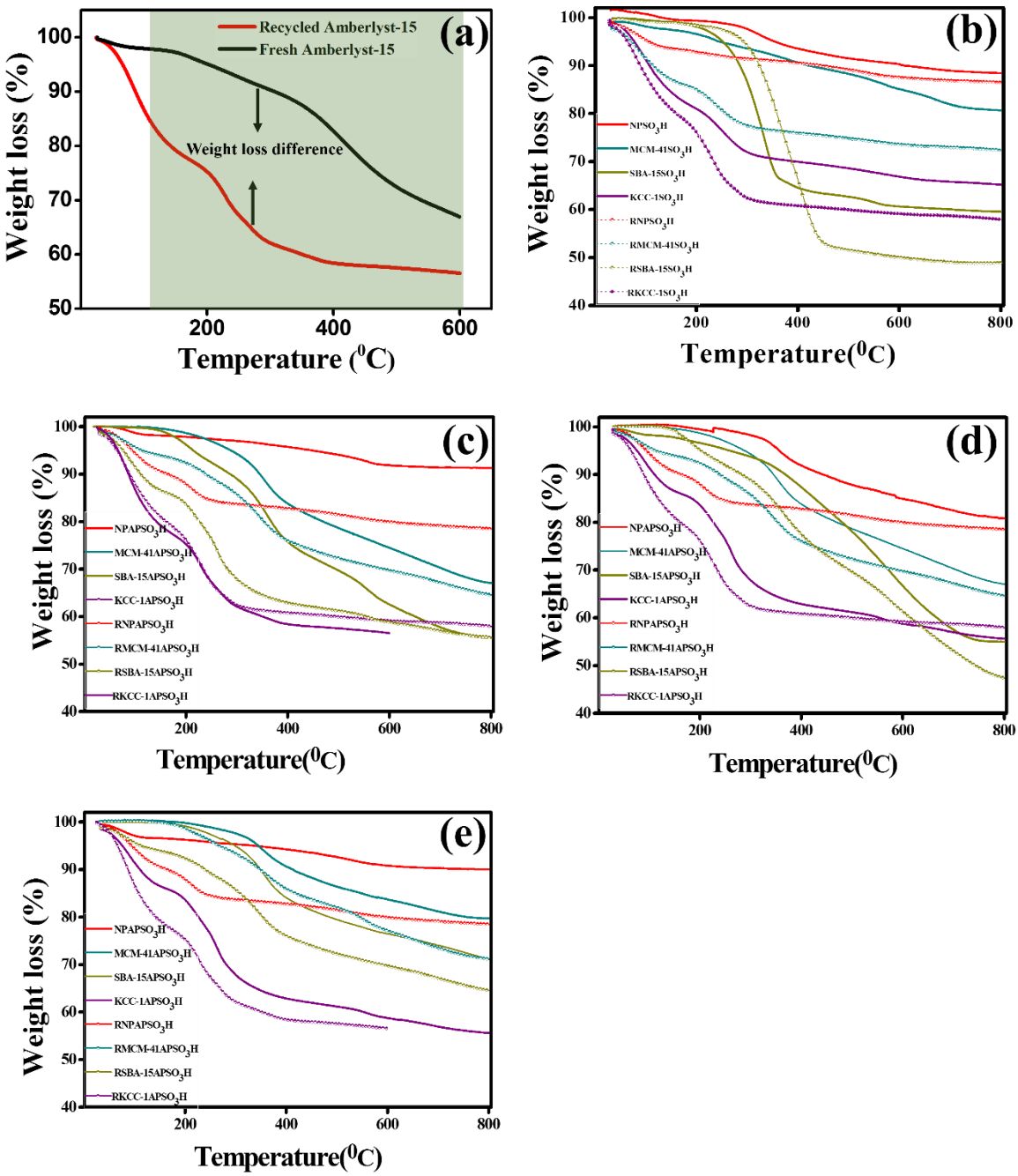

Figure S14: TGA diagram of fresh and recycled Amberlyst-15 from self-condensation of 2-MF (a), recycled silica supported catalysts from self-condensation of 2-MF (b), recycled silica supported catalysts from cross-condensation of 2-MF and FUR (c), recycled silica supported catalysts from cross-condensation of 2-MF and n-butanal (d) and recycled silica supported catalysts from cross-condensation of 2-MF and 2-pentanone (e).

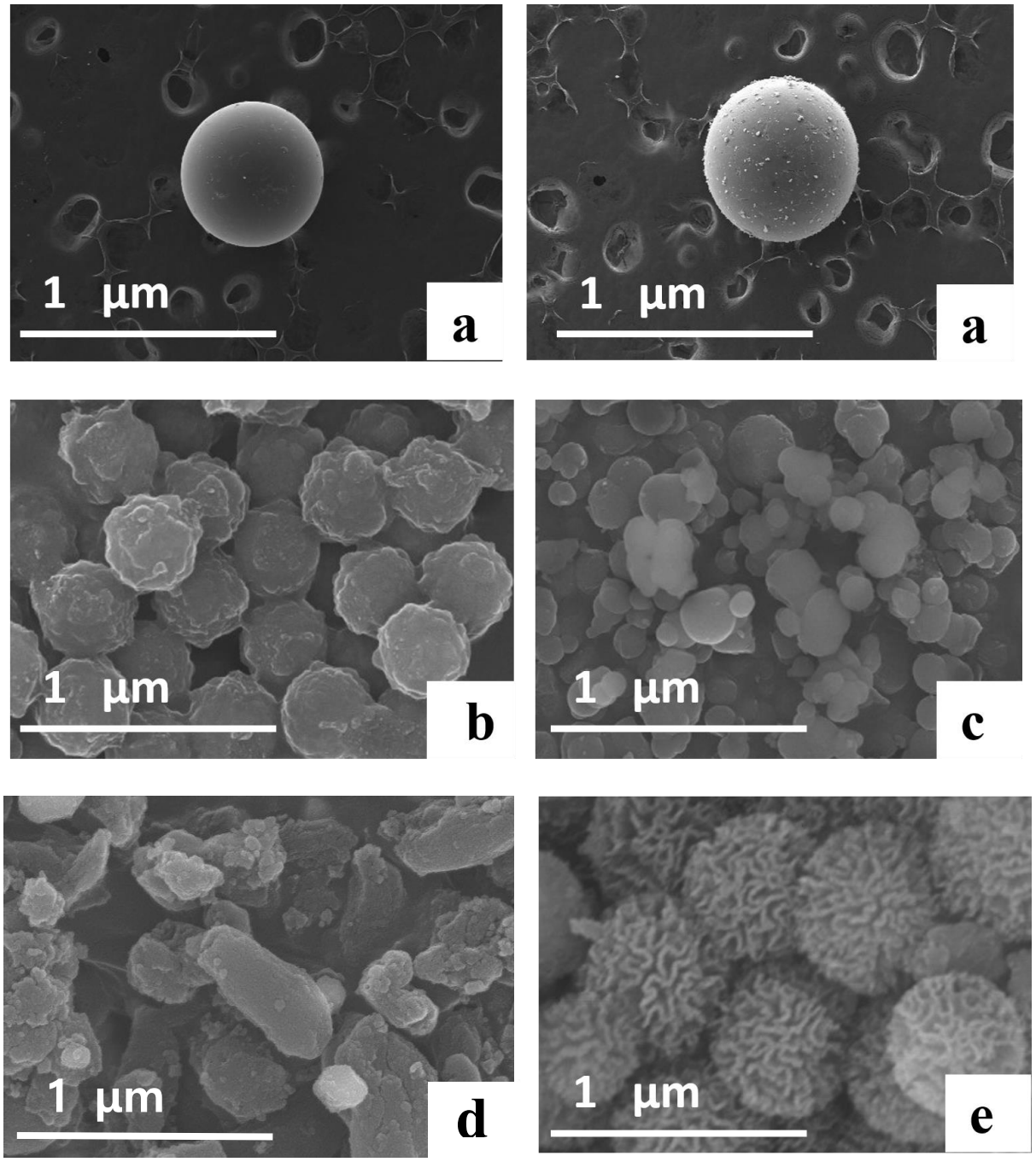

Figure S15: SEM images of Amberlyst-15 fresh and recycled (a), RNPSO$_3$H (b), RMCM-41SO$_3$H (c), RSBA-15SO$_3$H (d), and RKCC-1 SO$_3$H (e).

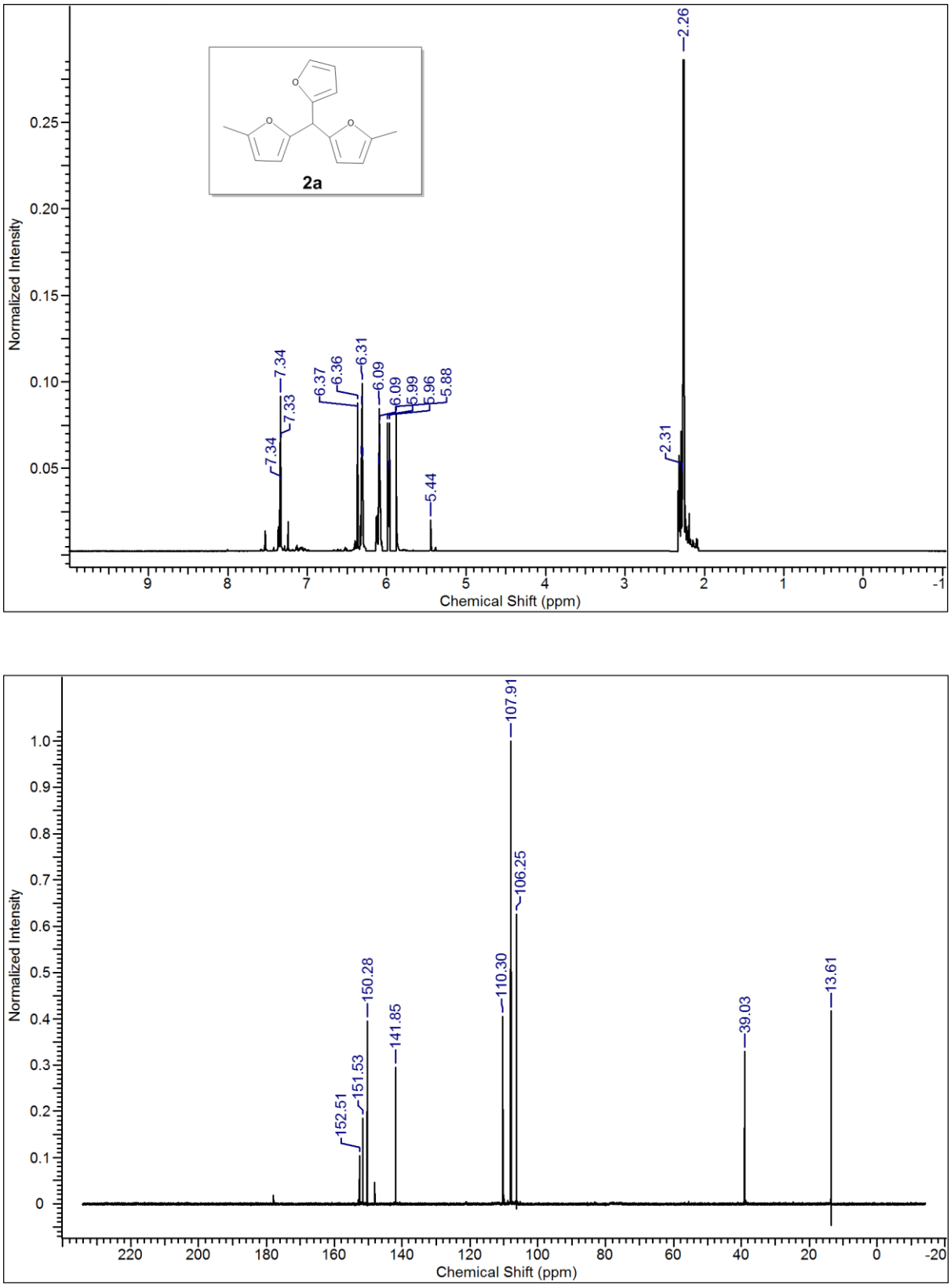

Figure S16: ^{1}H and ^{13}C NMR spectra of the 2a produced by the cross -condensation of 2-MF and FUR.

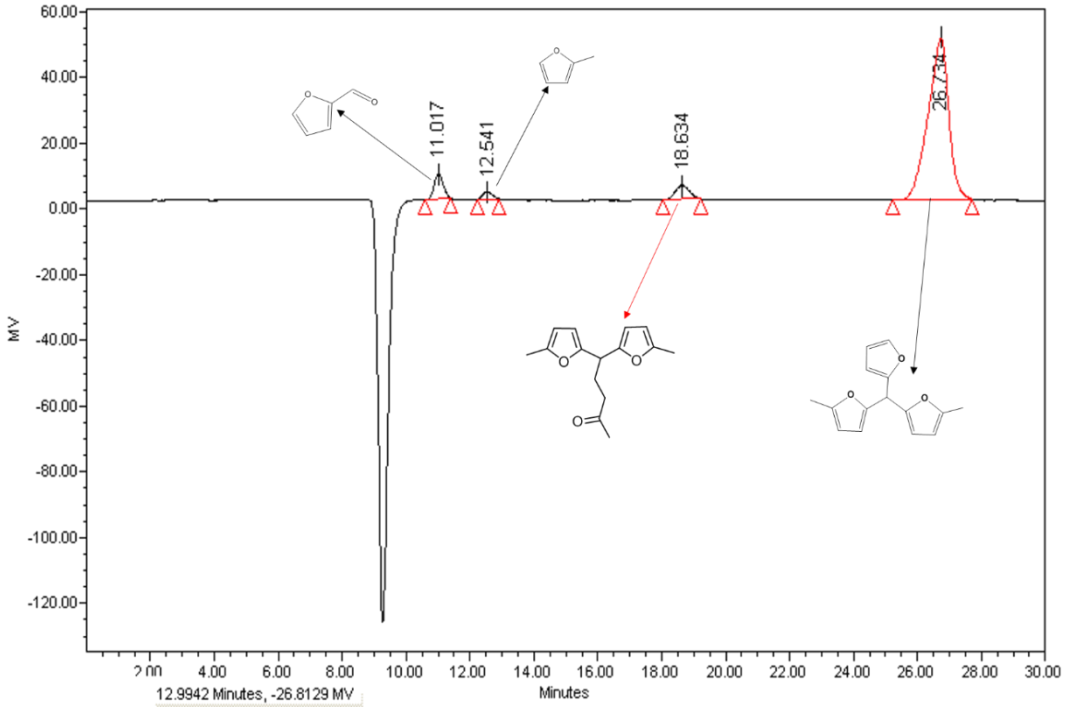

Figure S17: HPLC chromatogram of the liquid products from the cross-condensation of 2-MFand FUR

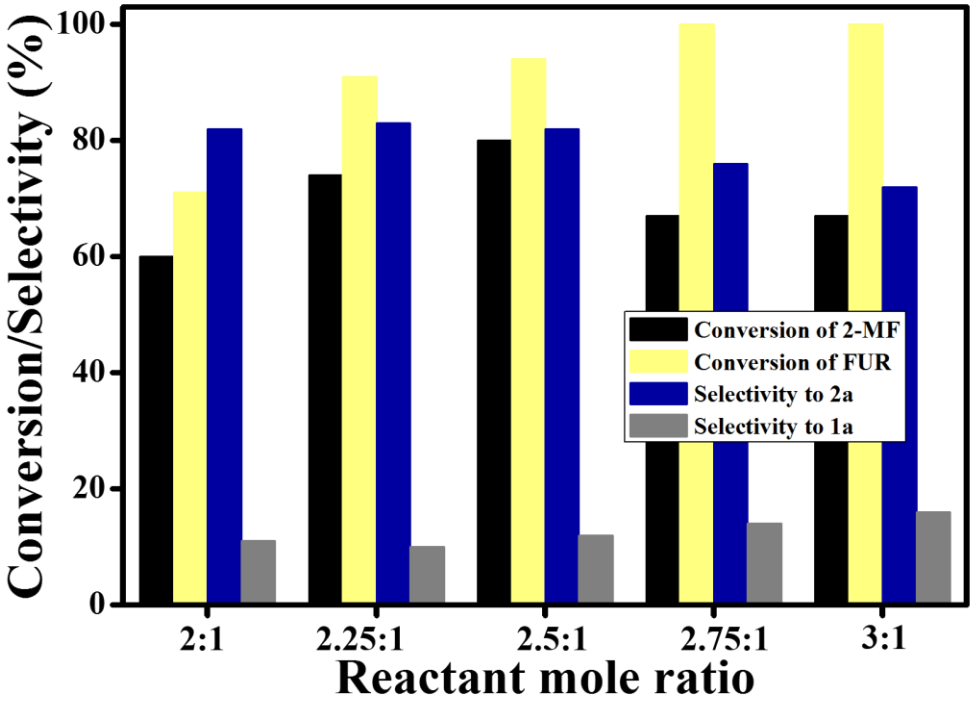

Figure S18: Result of the molar ratio study of the cross-condensation reaction of 2-MF and FUR using Amberlyst-15 catalysts for 2 h at 70 ^{0}C.

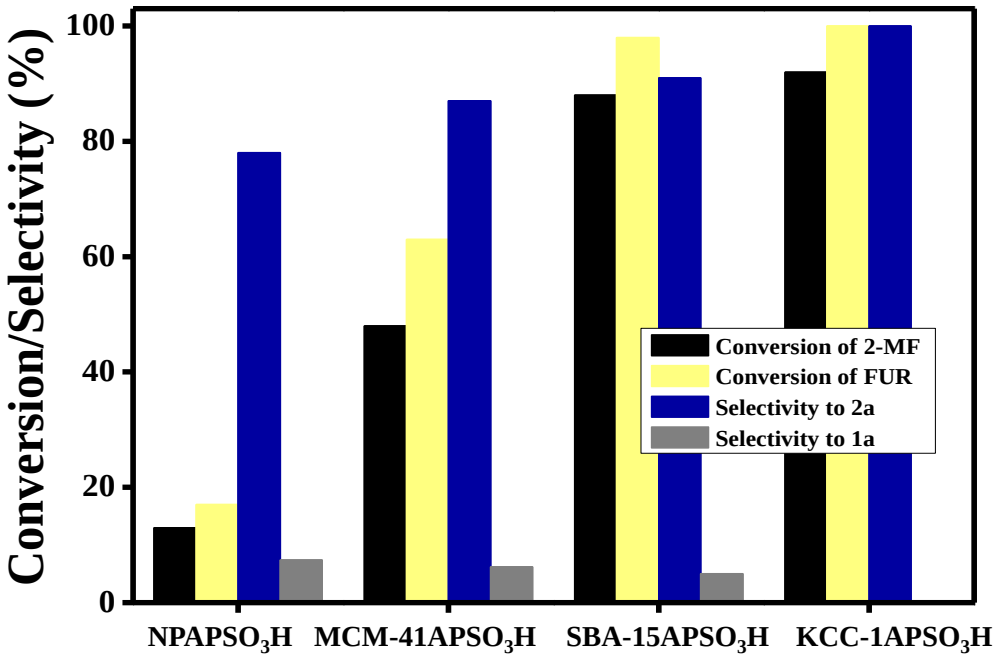

Figure S19: The effect of support morphology on conversion and selectivity. 2-MF (3.7 g), FUR (1.93 g) and catalyst (3 wt% by mass of 2-MF) were condensed for 2 h at 70 ^{0}C.

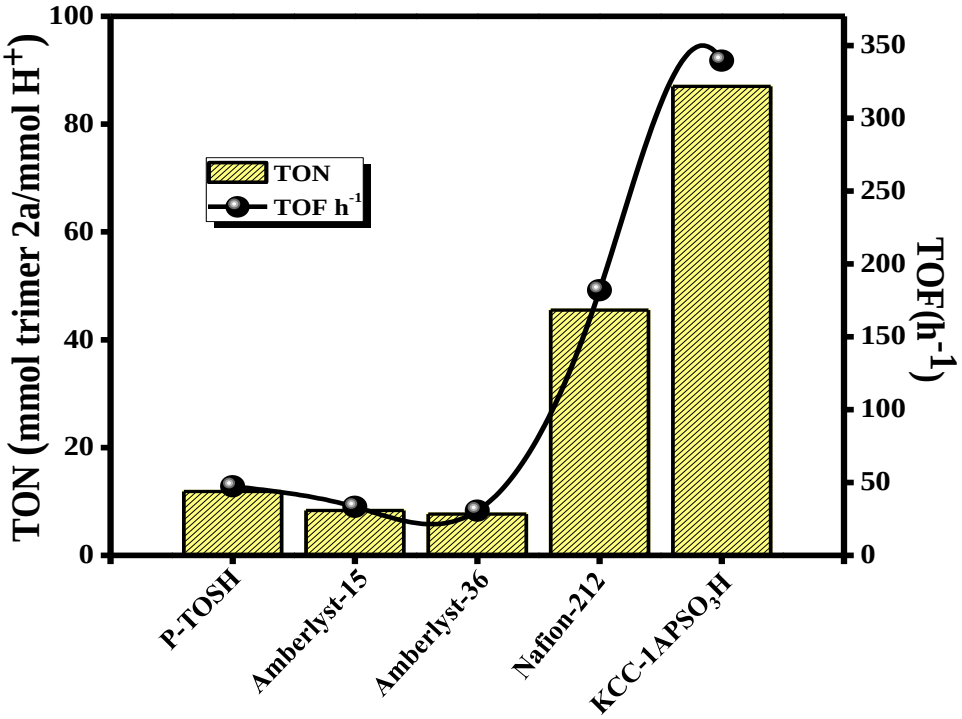

Figure S20: TON and TOF calculated from the yield after 0.25 h reaction. 2-MF (3.7 g), FUR (1.93 g) and catalyst (5 wt% by mass of 2-MF) were condensed for 2 h at 70 ^{0}C.

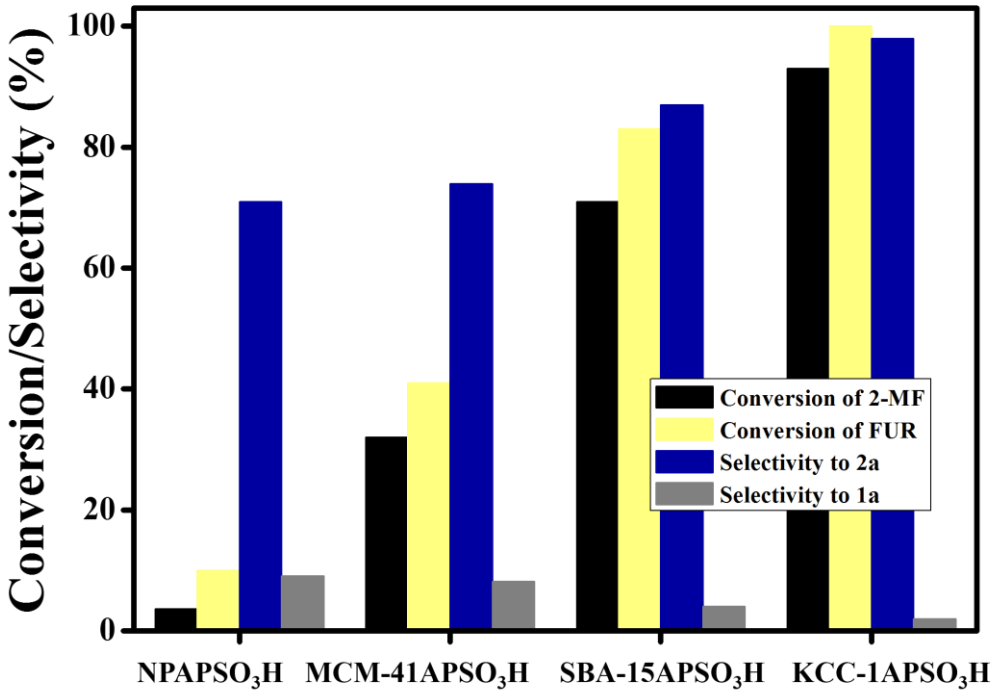

Figure S21: Result of the cross-condensation reaction of 2-MF and FUR using recycled NP, MCM-41, SBA-15 and KCC-1 supported catalysts. 2-MF (3.7 g), FUR (1.93 g) and catalyst (5 wt% by mass of 2-MF) were condensed for 2 h at 70 ^{0}C.

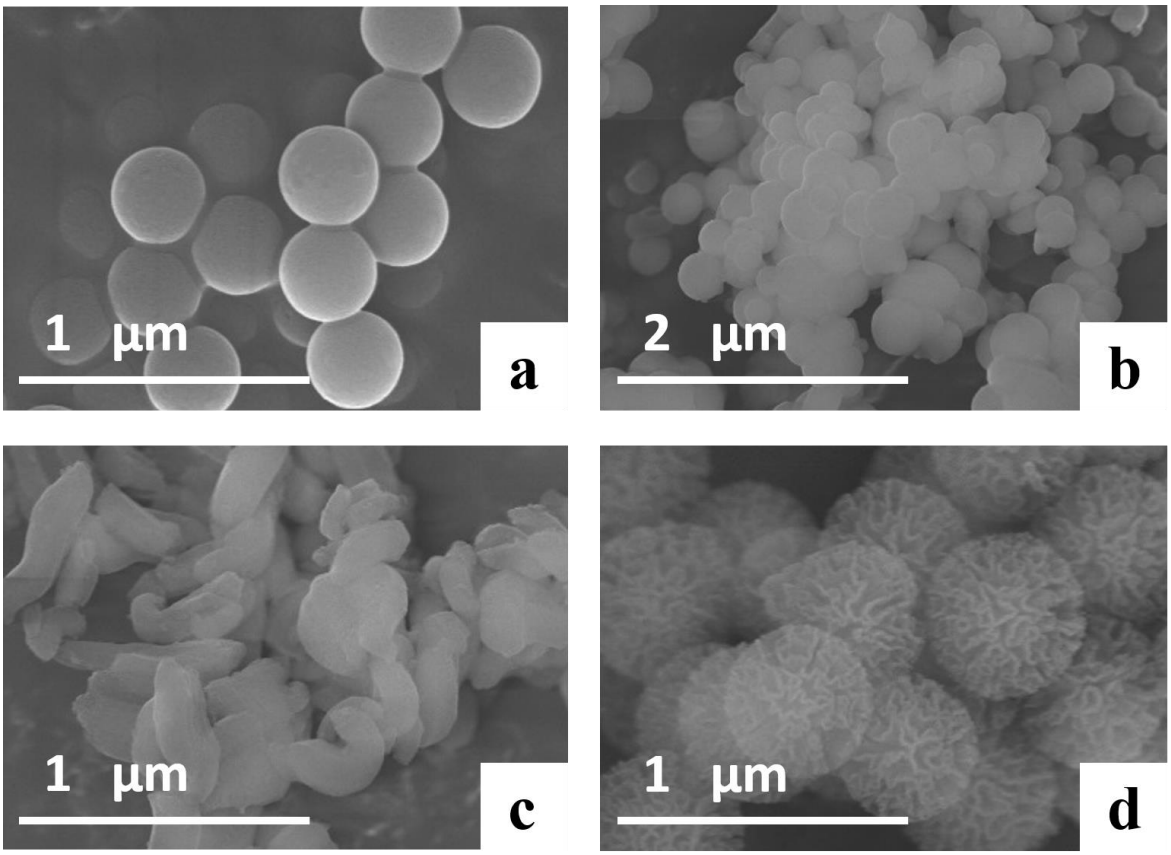

Figure S22: SEM images of recycled RNPAPSO$_3$H (a), RMCM-41APSO$_3$H (b), RSBA-15APSO$_3$H (c), and RKCC-1 APSO$_3$H (c).

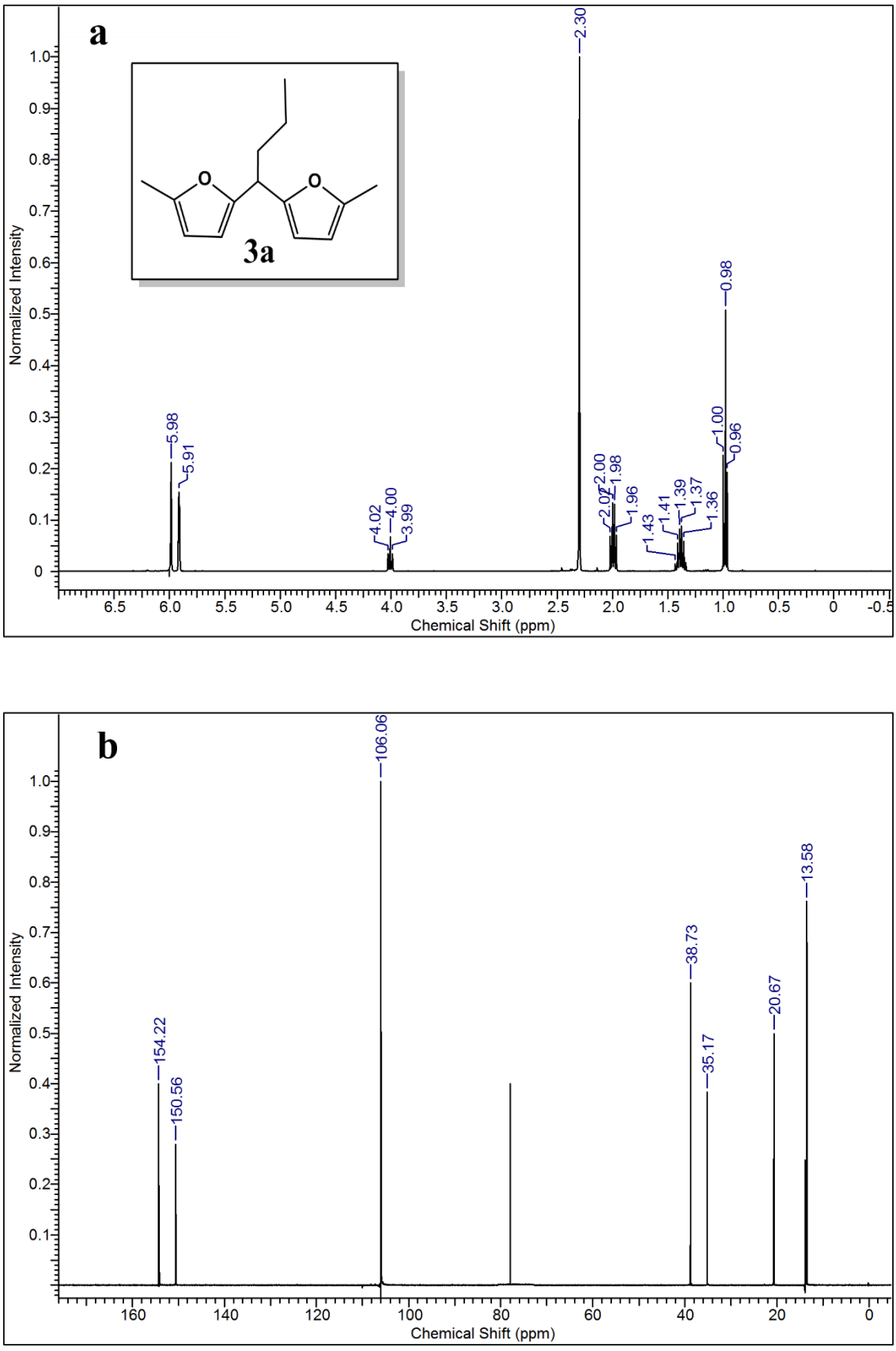

Figure S 23: ^{1}H and ^{13}C NMR spectra of the 3a produced by the cross -condensation of 2-MF and n-butanal.

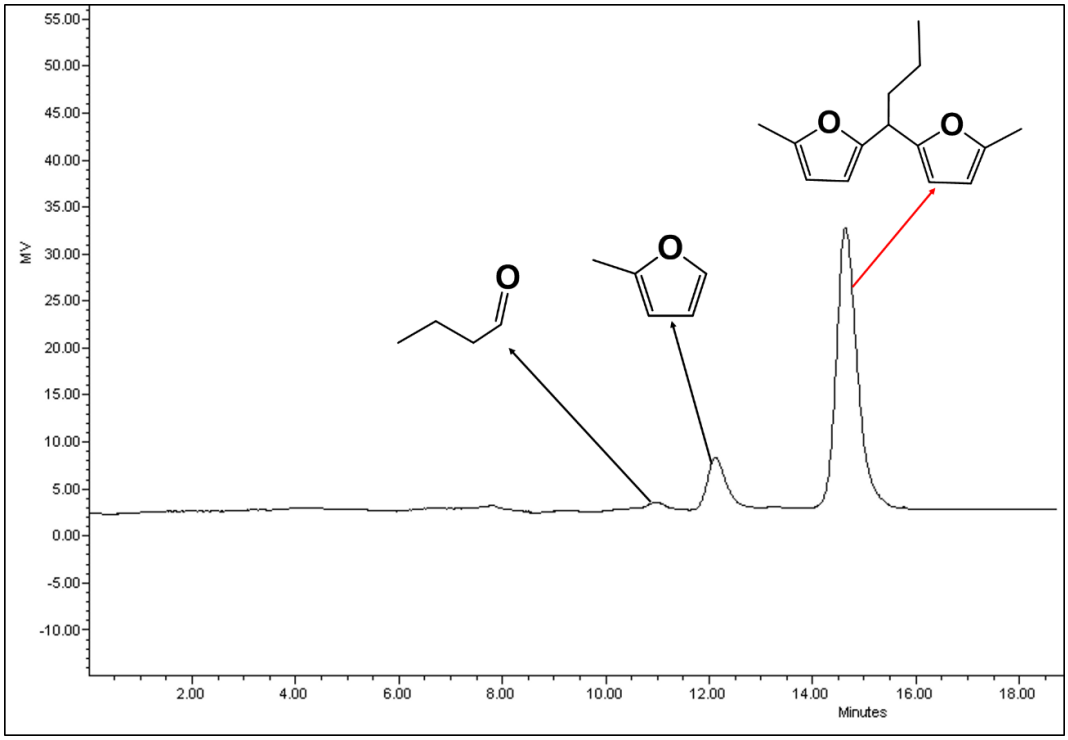

Figure S24: HPLC chromatogram of the liquid products from the cross-condensation of 2-MFand n-butanal.

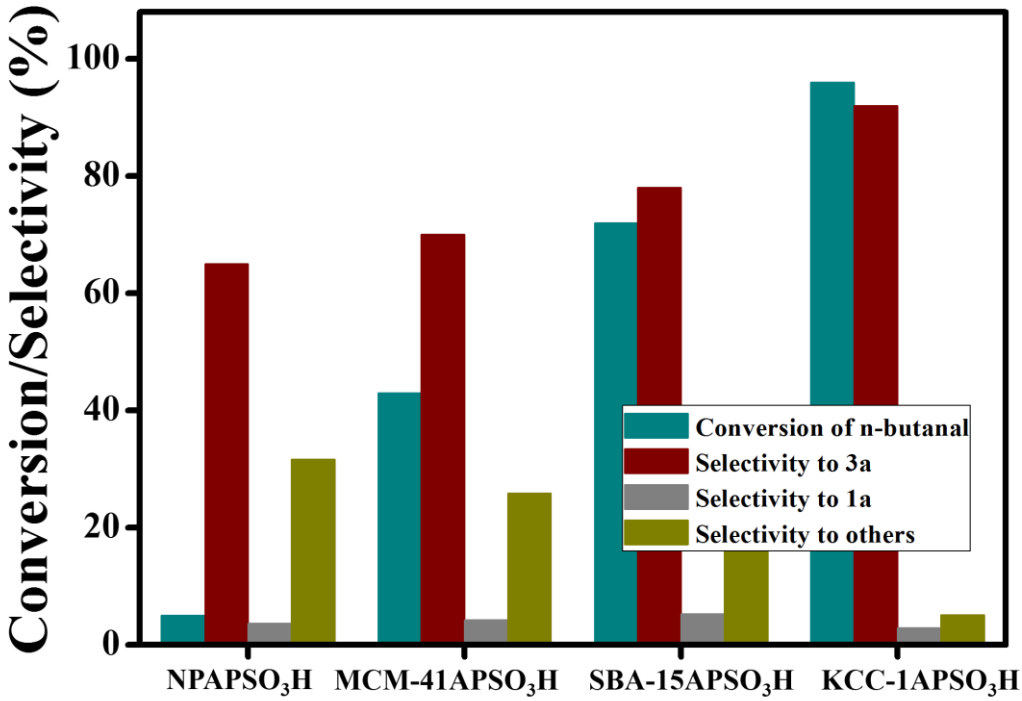

Figure S25: Result of the cross-condensation reaction of 2-MF and n-butanal using recycled NP, MCM-41, SBA-15 and KCC-1 supported catalysts. 2-MF (5 g), n-butanal (2.2 g) and catalyst (3 wt%) were condensed for 4 h at 50^0C.

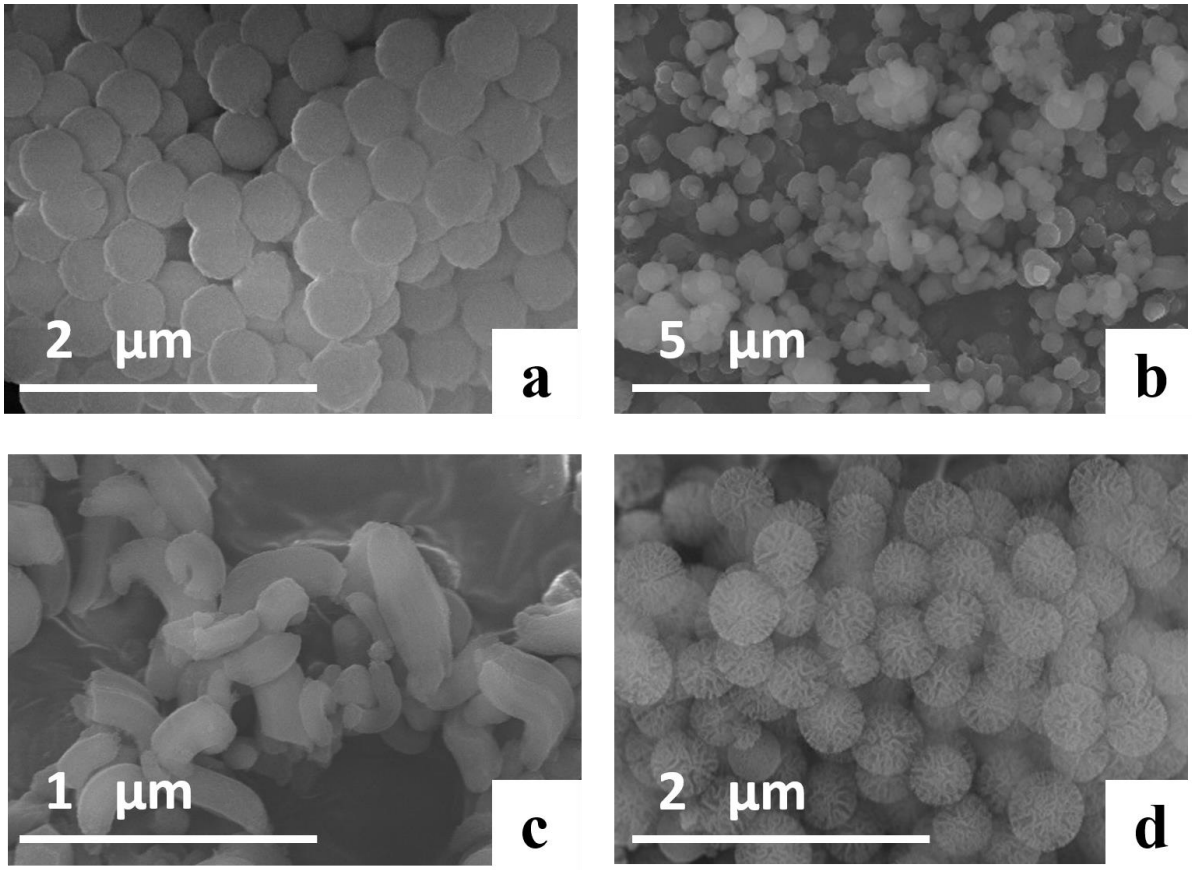

Figure S26: SEM images of recycled RNPAPSO$_3$H (a), RMCM-41APSO$_3$H (b), RSBA-15APSO$_3$H (c), and RKCC-1 APSO$_3$H (d).

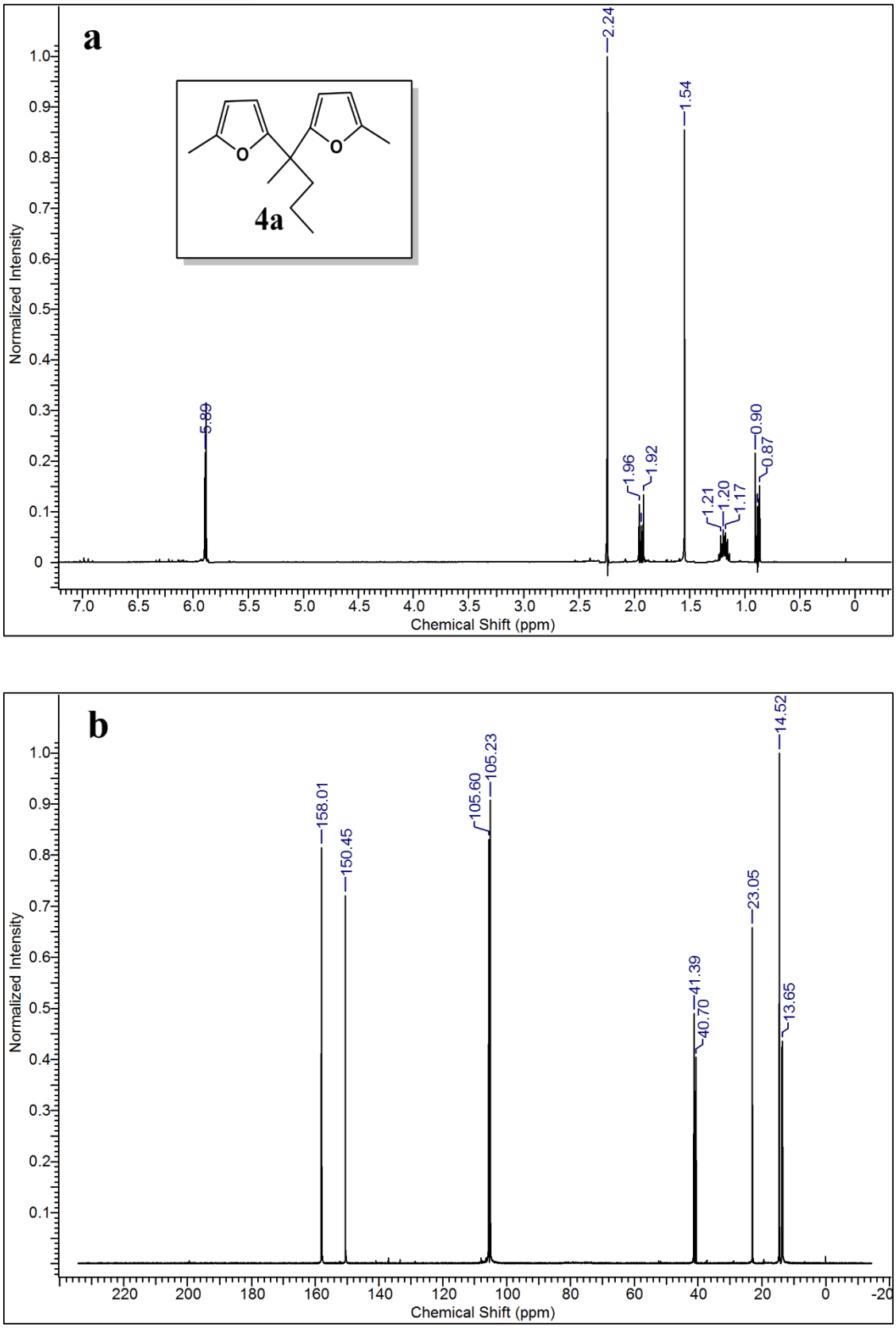

Figure S27: ^{1}H and ^{13}C NMR spectra of the 4a produced by the cross -condensation of 2-MF and 2-pentanone.

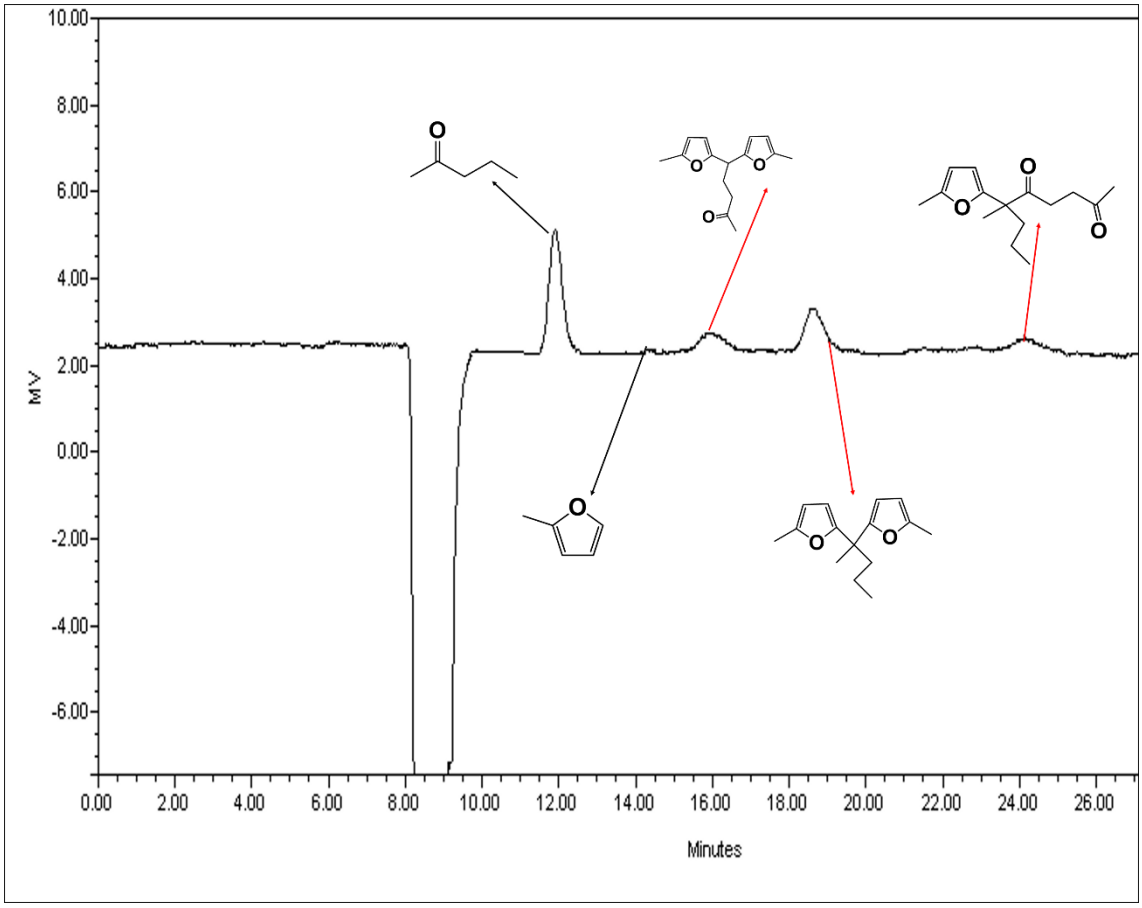

Figure S28: HPLC chromatogram of the liquid products from the cross-condensation of 2-MFand 2-pentanone.

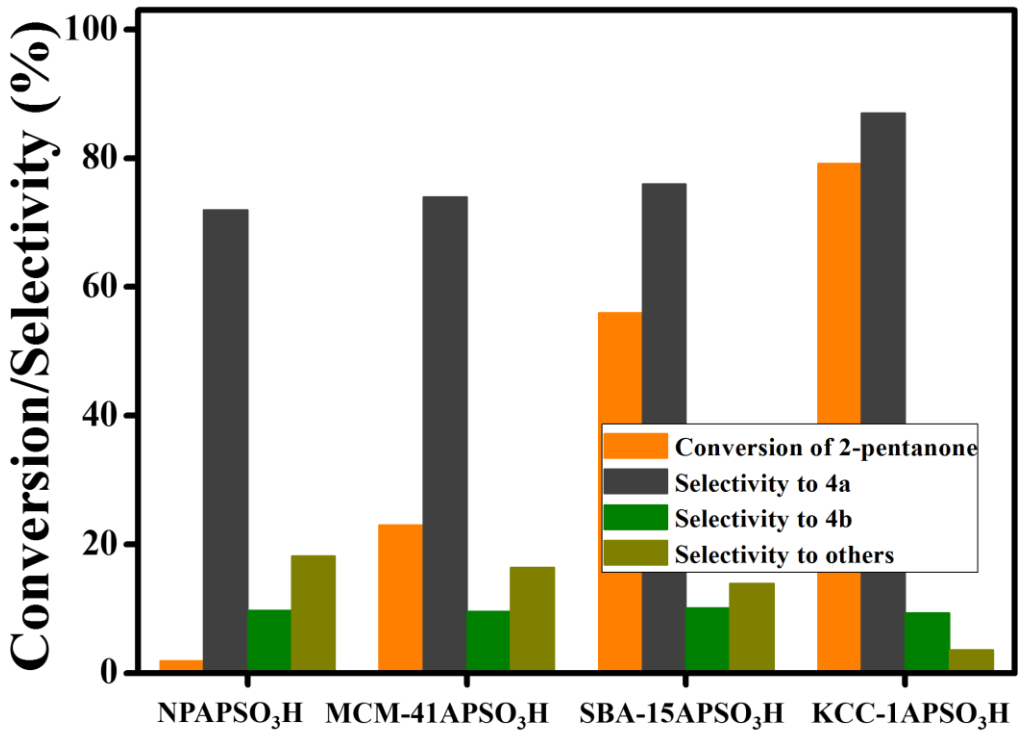

Figure S29: Result of the cross-condensation reaction of 2-MF and 2-pentanone using recycled NP, MCM-41, SBA-15 and KCC-1 supported catalysts. 2-MF (5 g), 2-pentanone (2.6 g) and catalyst (3 wt %) were condensed for 6 h at 85 ^{0}C.

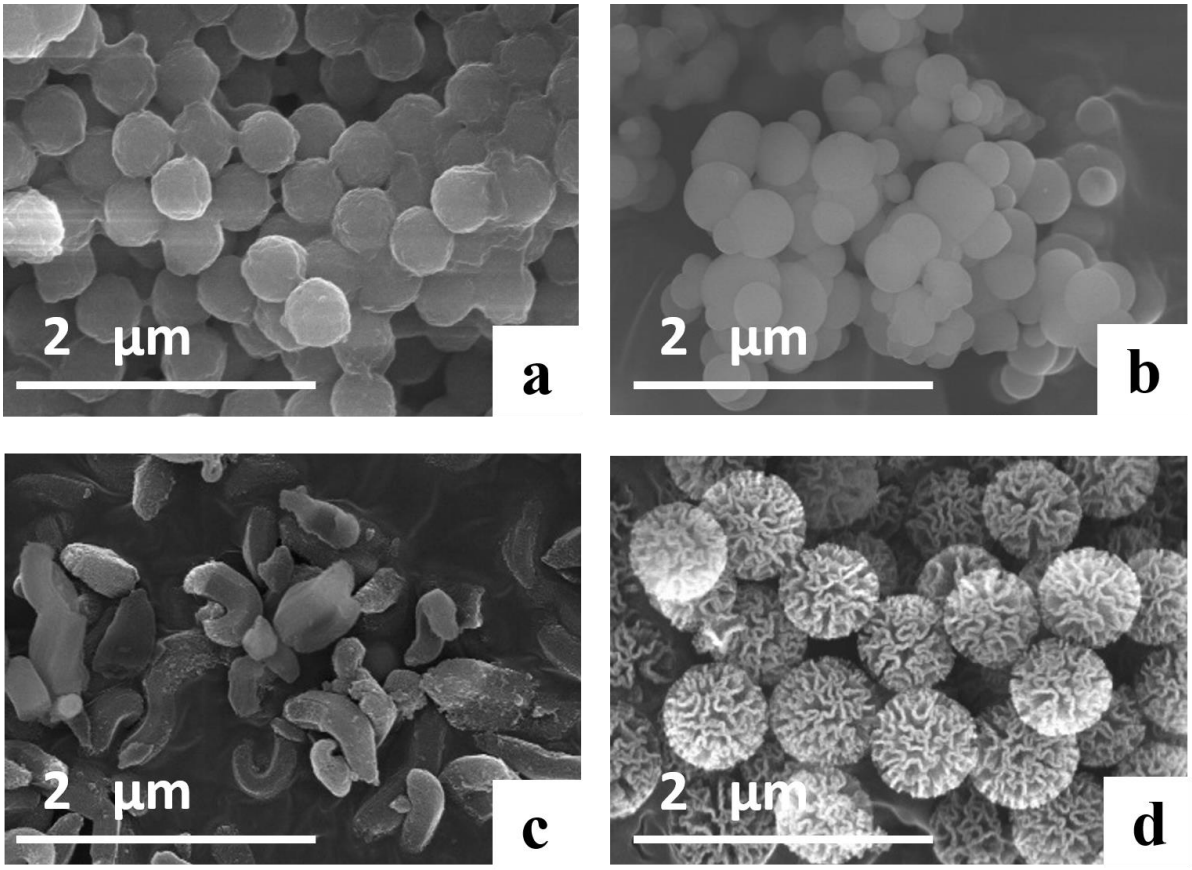

Figure S30: SEM images of recycled RNPAPSO$_3$H (a), RMCM-41APSO$_3$H (b), RSBA-15APSO$_3$H (c), and RKCC-1 APSO$_3$H (d).

Table S3: Comparison of the results acquired from this study with the previously reported values.

Self-condensation reaction							
Entry	**Catalyst**	**Temp. (^{0}C)**	**Time (h)**	**Conversion (%)**	**Selectivity 1a (%)**	**Selectivity 1b (%)**	**Ref.**
1	24 wt % H_2SO_4	85	3	45	86.8	NA	[1]
2	p-TosOH	85	3	37	NA	83.1	[1]
3	Amberlyst-15 with 15wt% H_2O	85	52	55.4	91	3.2	[1]
4	**KCC-1SO_3H with 10 wt% H_2O**	**85**	**48**	**60**	**100**	**0**	**This work**

Cross-condensation reaction of 2-methylfuran and furfural								
Entry	**Molar ratio**	**Catalyst (Wt %)**	**Temp. (^{0}C)**	**Time (h)**	**Conversion (%)**	**Yield /Selectivity 2a (%)**	**Yield/Selectivity 1a (%)**	**Ref.**
1	2:1	Nafion-212	50	2	80 (FUR)	67 (yield)	NA	[2]
2	2.2:1	Silica-supported alkyl sulfonic acid-functionalized catalyst	65	2	100 (FUR)	88.2 (yield)	NA	[3]
3	2:1	Lignosulfonate-based acidic resin	50	2	70.4 (2-MF)	65.4 (yield)	NA	[4]
4	2:1	$Pd/NbOPO_4$	80	5	92.3 (FUR)	89.7 (yield)	1.6	[5]
5	2.2:1	Improved graphene oxide carbocatalyst	60	3	100 (2-MF)	95 (yield)	NA	[6]
6	**2:1**	**KCC-1$APSO_3H$**	**70**	**2**	**100 (FUR)**	**100 (selectivity)**	**0**	**This work**

NA- not available

Cross-condensation reaction of 2-methylfuran and n-butanal							
Entry	**Molar ratio**	**Catalyst (Wt %)**	**Temp. (^{0}C)**	**Time (h)**	**Conversion (%)**	**Yield/Selectivity 3a (%)**	**Ref.**
1	2:1	*para*-toluenesulfonic acid	50	6	85 (n-Butanal)	91 (selectivity)	[7]
2	3:1				90 (n-Butanal)	93 (selectivity)	
3	3.5:1				93 (n-Butanal)	95 (selectivity)	
4	2:1	Nafion-212	50	4	96.6 (2-MF)	88.4 (yield)	[8]
5	2:1	Lignosulfonate-based acidic resin	50	2	78 (2-MF)	76 (yield)	[4]
6	**2:1**	**KCC-1$APSO_3H$**	**50**	**4**	**100 of n-Butanal**	**94 (selectivity)**	**This work**

Cross-condensation reaction of 2-methylfuran and 2-pentanone								
Entry	**Molar ratio**	**Catalyst (Wt %)**	**Temp. (^{0}C)**	**Time (h)**	**Conversion (%)**	**Selectivity 4a (%)**	**Selectivity 1a (%)**	**Ref.**
1	2.5:1	p-TosOH (3.8)	60	22.5	63 (2-pentanone)	76	11	[7]
2	2.5:1	p-TosOH (2.6)	100	3	76 (2-pentanone)	67	15	
3	2.5:1	H_2SO_4 (22.4)	60	9.5	61 (2-pentanone)	22	46	
4	3:1	H_2SO_4 (22.4)	100	1	71 (2-pentanone)	14	55	
5	**2.5:1**	**KCC-1$APSO_3H$**	**85**	**6**	**89 (2-pentanone)**	**82**	**10.2**	**This work**

1 I. Yati, M. Yeom, J. W. Choi, H. Choo, D. J. Suh and J. M. Ha, *Appl. Catal. A Gen.*, , DOI:10.1016/j.apcata.2015.02.002.

2 G. Li, N. Li, Z. Wang, C. Li, A. Wang, X. Wang, Y. Cong and T. Zhang, *ChemSusChem*, 2012, **5**, 1958–1966.

3 M. Balakrishnan, E. R. Sacia and A. T. Bell, *ChemSusChem*, 2014, **7**, 1078–1085.

4 S. Li, N. Li, G. Li, L. Li, A. Wang, Y. Cong, X. Wang and T. Zhang, *Green Chem.*, , DOI:10.1039/C5GC00372E.

5 Q. Xia, Y. Xia, J. Xi, X. Liu, Y. Zhang, Y. Guo and Y. Wang, *ChemSusChem*, 2017, **10**, 747–753.

6 S. Dutta, A. Bohre, W. Zheng, G. R. Jenness, M. Núñez, B. Saha and D. G. Vlachos, *ACS Catal.*, 2017, **7**, 3905–3915.

7 A. Corma, O. de la Torre and M. Renz, *Energy Environ. Sci.*, , DOI:10.1039/c2ee02778j.

8 G. Li, N. Li, J. Yang, A. Wang, X. Wang, Y. Cong and T. Zhang, *Bioresour. Technol.*, , DOI:10.1016/j.biortech.2013.01.116.